Development of Efficient and Accurate Skeletal Mechanisms for Hydrocarbon Fuels and Kerosene Surrogate

Fengquan Zhong[1], Sugang Ma, Xinyu Zhang
State Key Laboratory of High Temperature Gas Dynamics, Institute of Mechanics, Chinese Academy of Sciences, Beijing, China

Chih-Jen Sung
Department of Mechanical Engineering, University of Connecticut, Storrs, Connecticut, USA

Kyle E. Niemeyer
School of Mechanical, Industrial, and Manufacturing Engineering, Oregon State University, Corvallis, Oregon, USA

Abstract In this paper, the methodology of the directed relation graph with error propagation and sensitivity analysis (DRGEPSA), proposed by Niemeyer et al. [Combustion and Flame 155 (2010) 1760–1770], and its differences to the original directed relation graph method are described. Using DRGEPSA, the detailed mechanism of ethylene containing 71 species and 395 reaction steps is reduced to several skeletal mechanisms with different error thresholds. The 25 species and 131 steps mechanism and the 24 species and 115 steps mechanism are found to be accurate for the predictions of ignition delay time and laminar flame speed. Although further reduction leads to a smaller skeletal mechanism with 19 species and 68 steps, it is no longer able to represent the correct reaction processes. With the DRGEPSA method, a detailed mechanism for n-dodecane considering low-temperature chemistry and containing 2115 species and 8157 steps is reduced to a much smaller mechanism with 249 species and 910 steps while retaining good accuracy. If considering only high-temperature (higher than 1000 K) applications, the detailed mechanism can be simplified to even smaller mechanisms with 65 species and 340 steps or 48 species and 220 steps. Furthermore, a detailed mechanism for a kerosene surrogate having 207 species and 1592 steps is reduced with various error thresholds and the results show that the 72 species and 429 steps mechanism and the 66 species and 392 steps mechanism are capable of predicting correct combustion properties compared to those of the detailed mechanism. It is well recognized that kinetic mechanisms can be effectively used in computations only after they are reduced to an acceptable size level for computation capacity and at the same time retaining accuracy. Thus, the skeletal mechanisms generated from the present work are expected to be useful for the application of kinetic mechanisms of hydrocarbons to numerical simulations of turbulent or supersonic combustion.

Keywords: reduced chemistry, hydrocarbons, directed relation graph, ignition delay time

1 Introduction

[1]Corresponding author
No.15 Beisihuanxi Road, Institute of Mechanics, Chinese Academy of Sciences, 100190, Beijing, China
Email: fzhong@imech.ac.cn

Hydrocarbons have been widely used to provide energy and power in many engineering applications and their combustion properties are one of the most critical technical issues. Reactions of hydrocarbons, especially with those with large molecules, consist of, e.g., the thermal decomposition of paraffins and cycloalkanes and the formation of alkyl radicals, reactions with oxygen atoms and generation of formyl radicals, formation of carbon monoxide and carbon dioxide, and low temperature reaction routes. Therefore, kinetic mechanisms must contain sufficient numbers of species and elementary reactions for an accurate prediction of reaction processes, ignition and extinction properties, flame propagation, and pollutant formation. The number of species and reaction steps for a comprehensive detailed mechanism of hydrocarbons usually reaches hundreds or even thousands, so the direct application of detailed mechanisms in computational fluid dynamics (CFD) simulations becomes infeasible. For example, the detailed mechanism for ethylene proposed by Wang and Laskin [1] includes 71 species and 395 reaction steps; the size of the mechanism for n-heptane developed by Curran et al. [2], however, increases to 561 species and 2539 steps, respectively. For hydrocarbons with large molecules such as n-dodecane, the size of detailed mechanism is even bigger! The mechanism published by Westbrook et al. [3] for n-alkanes, comprised of 2115 species and 8157 reaction steps, cannot be practically implemented in CFD codes for even two-dimensional turbulent flow problems. Detailed mechanisms of hydrocarbons with hundreds or thousands of species and steps cause a significant increase in the computational cost for the solution of the governing equations (species and energy conservation equations), becoming a bottleneck for numerical simulation of reacting flows. At the same time, the so-called "stiffness" [4] due to variations in characteristic times of elementary reaction steps leads to low efficiency in the temporal convergence of the solution, resulting in further significant increase in the computational cost. Hence, it has been shown that reduction of a detailed reaction mechanism into a simpler and smaller one that is acceptable for CFD simulations is one of the key issues for numerical modeling of chemically reacting flows.

In the recent twenty years, the reduction methods for chemical kinetic mechanisms have been continuously developed, as reviewed recently by Lu and Law [5] and Pope [6] in the context of turbulent combustion modeling. Sensitivity analysis (SA) is one of the earliest methods [e.g., 7, 8]. The basic idea of SA is to analyze how the change in the species fractions would affect key parameters of the reaction system such as, e.g., ignition delay time or the formation rates of radicals, to determine the relative importance of species, and the unimportant species and reaction steps are then eliminated. The SA method still retains many species and steps and its reduction efficiency is relatively low, especially for large reaction mechanisms. The computational singular perturbation (CSP) method proposed by Lam [9] analyzes the Jacobian matrix of the species rate equations and identifies the species which contribute to fast and slow processes in the reaction system. Similar to the SA method, reduced or skeletal mechanisms obtained with CSP are still relatively large and other reduction processes are usually required for further reductions. The reduction methods based on quasi-steady state (QSS) assumption developed by Peters [10] and Chen [11] have also been widely used. The QSS method, however, needs to compute the local concentrations of the quasi-steady species in terms of molar fractions of the other species and local temperature and pressure via complex matrix operations [cf. 12, 13]. Calculation of large-size matrices would slow down the computation and affect stability of the numerical scheme. To the authors' experiences in the usage of QSS method, the reduction in the species number is not proportional to the rate of speed-up of the computation, and for turbulent combustion modeling with large fluctuations, the stability of numerical scheme would diminish and the solution converges much slower. Meanwhile, other methodologies such as dimension reduction or tabulation

have been developed to accelerate reactive-flow simulations, e.g., the work of Pope and coworkers [14–16].

The directed relation graph (DRG) method was proposed by Lu and Law [17] for efficient mechanism reduction. Based on a directed graph representing interdependence of species in the mechanism, the DRG method evaluates the contribution of other species on the production or consumption rate of the pre-set target species and deletes species with weak contributions. The detailed procedure of DRG and its reduction performance can be found in the literature [17–19]. The DRG method has very high reduction efficiency especially for large-size reaction mechanisms. Pepiot-Desjardins and Pitsch [20] modified the original DRG method and developed the directed relation graph with error propagation (DRGEP) method. Instead of only emphasizing the importance of single graph edges like DRG, the DRGEP method considers propagation of the induced error along the graph paths and evaluates the overall importance of all the species to the target species. The DRGEP method [20–22] improves the effectiveness of mechanism reduction for a given accuracy level compared to the DRG method. Recently, Niemeyer et al. [21] proposed a method of DRGEP with sensitivity analysis (DRGEPSA), in which sensitivity analysis of certain remaining species is conducted after the DRGEP phase. It was shown that DRGEPSA produces more compact skeletal mechanisms for the same level of accuracy compared to DRG or DRGEP alone [21].

In addition to a priori skeletal mechanism reduction techniques that generate a single mechanism for use throughout an entire simulation, recently adaptive or dynamic mechanism reduction techniques, typically employing methods such as DRG and DRGEP, have been demonstrated. For example, Liang et al. [23, 24] developed one of the first such dynamic reduction methods using DRGEP, followed by the efforts of Yang et al. [25], Shi et al. [26], and Ren et al. [27]. Significant speed-ups in the computation of reacting flows can be achieved using such an approach, although the issue of a priori error control remains a challenge.

In this paper, the main process of DRGEPSA and its differences to the original DRG will first be addressed. Using DRGEPSA, a detailed mechanism for ethylene with 71 species and 395 reaction steps proposed by Wang and Laskin [1] is reduced with varied accuracy levels. The resulting skeletal mechanisms are examined based on the comparison of ignition delay times and laminar flame speeds determined with the skeletal mechanism, the detailed mechanism, and literature experimental data. In addition, reductions of reaction mechanisms for large hydrocarbon fuels such as n-dodecane and a kerosene surrogate are conducted. The detailed mechanism of C_8–C_{16} n-alkanes—including low-temperature chemistry—developed by Westbrook et al. [3] is reduced into several skeletal mechanisms with varying levels of accuracy and applicable temperature ranges. The 207 species and 1592 reaction steps mechanism for a three-species surrogate for kerosene, a mixture of n-decane (74%), n-propylbenzene (15%), and n-propylcyclohexane (11%) in volume, introduced by Dagaut [28], is also reduced. It will be shown in due course that skeletal mechanisms with 72 species/429 steps and 66 species/392 steps are obtained with satisfactory accuracy. The present work is expected to provide foundations for integrating realistic chemistry of hydrocarbons into large-scale turbulent or supersonic combustion modeling.

2. Methodology of DRGEPSA

The key features of DRGEP are first introduced briefly in this section. For more detailed descriptions, please refer to the literature [20–22]. For a reaction system, the overall production rate of

species S_1 can be expressed as:

$$R_{S_1} = \sum_{i=1}^{N} \nu_{S_1,i}\omega_i \,, \tag{1}$$

where ω_i is the net reaction rate of the *i*-th reaction step that can be positive or negative, $\nu_{S_1,i}$ is the overall stoichiometric coefficient of S_1 for the *i*-th step, and *N* is the total number of the reaction steps in the reaction mechanism.

To evaluate quantitatively the dependency of another species S_2 on S_1, a non-dimensional coefficient r_{S_1,S_2}, the so-called "direct interaction coefficient" [cf., 20–22], is calculated as follows:

$$r_{S_1,S_2} = \frac{\left|\sum_{i=1}^{N} \nu_{S_1,i}\omega_i\delta_{S_2}^{i}\right|}{\max(P_1,P_2)}, \tag{2}$$

where $\delta_{S_2}^{i} = 1$ if the i-th reaction step involves species S_2, otherwise $\delta_{S_2}^{i} = 0$, $P_1 = \sum_{i=1}^{N} \max\left(0, \nu_{S_1,i}\omega_i\right)$ and $P_2 = \sum_{i=1}^{N} \max\left(0, -\nu_{S_1,i}\omega_i\right)$. P_1 and P_2 are the sums of the production and consumption rates, respectively, of the reaction steps involving species S_1.

Figure 1 shows a directed relation graph with various pathways between species A and E. As shown in the figure, the value given to the edge representing species relations such as A→B includes all the elementary reactions having both species A and B in either the products or reactants. In the DRG method [17–19], only the direct connections between species are used to determine the importance of species to the targets. In contrast, the DRGEP method considers species further away from targets to be less important, geometrically damping the importance through indirect graph edges. In addition to direct connections between species, such indirect relations (through interactions with other species) can be observed in the graph. Given below is the equation used to calculate $r_{AB,p}$, the so-called "path-dependent interaction coefficient" [20–22], which measures the dependence of species B to species A based on a certain path in the graph:

$$r_{AB,p} = \prod_{j=1}^{m} r_{S_j,S_{j+1}} \,. \tag{3}$$

There are in total three graph pathways between species A and E as shown in Fig. 1 and they are calculated as $r_{AE,1} = r_{A,B}r_{B,E}$, $r_{AE,2} = r_{A,E}$, $r_{AE,3} = r_{A,C}r_{C,D}r_{D,E}$.

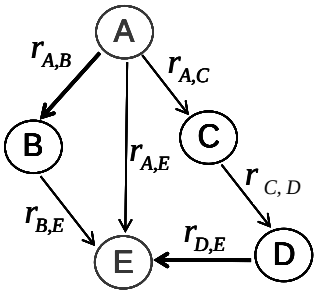

Fig. 1 A directed relation graph of species A and E

Next, the overall interaction coefficients, R_{AE}, for DRG and DRGEP can be respectively defined as:

$$R_{AE}^{DRG} = MAX(r_{A,B}, r_{B,E}, r_{A,E}, r_{A,C}, r_{C,E}, r_{D,E}) \tag{4}$$

and

$$R_{AE}^{DRGEP} = MAX(r_{AE,1}, r_{AE,2}, r_{AE,3}). \tag{5}$$

In the DRGEP method, R_{AE}^{DRGEP} is the overall importance measure for species, which considers propagation of the induced error along graph pathways. On the other hand, R_{AE}^{DRG} in the DRG method relies on the individual connections between species. Practically, R_{AE}^{DRGEP} is determined for all species through a graph search initiating at the target species, using Dijkstra's algorithm as demonstrated by Niemeyer and Sung [22].

The species E would be removed from the mechanism when $R_{AE}^{DRGEP} \le \varepsilon_{EP}$, where ε_{EP} is an error threshold. The value of ε_{EP} can be given a priori (e.g., approximately 0.001), or it can be automatically determined by comparing the ignition delay times calculated with the parent detailed mechanism and the resulting skeletal mechanism over a range of conditions (in terms of temperatures, pressures, and equivalence ratios) and iterating based on a pre-set error limit δ_{EP} [21].

The mechanism reduced by DRGEP can be further analyzed with sensitivity analysis; see [21] for details. Using $\varepsilon_{EP} < R_{AE} < \varepsilon^*$ (where the upper threshold ε^* is set as 0.1 for all the present cases [21]), limbo species can be identified for the brute-force sensitivity analysis [21, 29]. Briefly, limbo species are removed one-by-one and the errors induced by their individual removal are evaluated. Then, these induced errors are used to sort the species for removal, and species are removed in this order until the error reaches the user-defined limit.

3. Results and discussions

3.1 Skeletal mechanisms of ethylene

The reduction of a detailed ethylene mechanism is first discussed. The detailed mechanism developed by Wang and Laskin [1] includes 71 species and 395 reaction steps. Comparisons of ignition delay times and laminar flame speeds calculated with the detailed mechanism and experimental data (ignition delay times taken from Saxena et al. [30], with laminar flame speeds taken from Gibbs and

Calcote [31] and Egolfopoulos et al. [32]) demonstrate the accuracy of the detailed mechanism.

With a stoichiometric ethylene/air mixture, an input temperature range of 1100–1500 K, an input pressure of 1 atm, and the error limit δ_{EP} set as 30% (resulting in ε_{EP} = 0.03 determined iteratively), the detailed mechanism is reduced to a skeletal mechanism containing 25 species and 131 reaction steps. Figure 2(a) compares the ignition delay times calculated by the detailed mechanism and this skeletal mechanism. The two curves almost overlap with each other and a maximum discrepancy of only 7% is observed. Moreover, Fig. 2(b) compares the laminar flame speed results. Similarly, this skeletal mechanism gives good predictions of laminar flame speeds with a maximum difference of only 5% over the range of conditions investigated. In Fig. 2(b), experimental data from Gibbs and Calcote [31] and Egolfopoulos et al. [32] are also plotted.

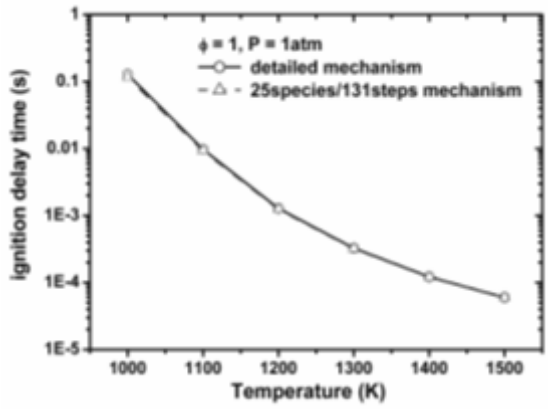

(a)

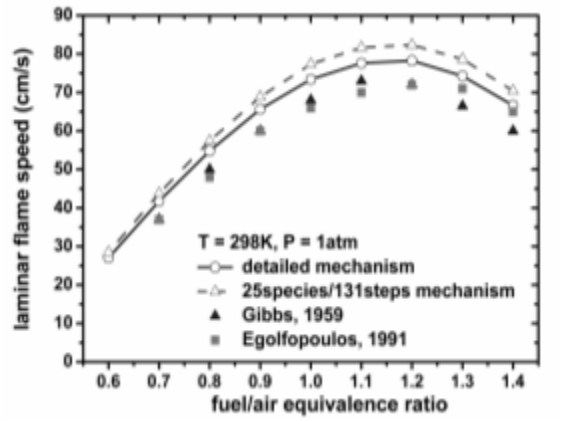

(b)

Fig. 2 Comparison of the detailed mechanism with the 25-species skeletal mechanism (a): ignition delay time; (b): laminar flame speed

Relaxing the error threshold ε_{EP} by limiting the temperature range further decreases the number of species and reaction steps, leading to skeletal mechanisms with 24 species and 115 steps (ε_{EP} = 0.038) and with 19 species and 68 steps (ε_{EP} = 0.163). Table 1 summarizes the species included in the three skeletal mechanisms generated herein.

Figure 3(a) presents the ignition delay times predicted by the detailed mechanism as well as the 24-species and 19-species skeletal mechanisms. From the comparison, it is found that the 24-species skeletal mechanism can give satisfactory results except in the high-temperature region (1400–1500 K), where a relatively large (but still accurate enough for numerical simulations) discrepancy of about 25% is observed. For the ignition delay time predictions using the 19-species skeletal mechanism, however, significant differences from those obtained using the detailed mechanism, especially in the temperature range of 1000–1100 K, are observed. Figure 3(b) further shows the results of laminar flame speed calculations. Similar to the ignition delay times, the 24-species skeletal mechanism has good accuracy in predicting laminar flame speeds over the conditions tested. On the other hand, the 19-species skeletal mechanism yields poor predictions, and even incorrectly predicts the overall trend in terms of the laminar flame speed variation with fuel/air equivalence ratio.

Table 1 Species of the resulting skeletal mechanisms for ethylene combustion

skeletal mechanism	retained species	deleted species	
25-species	H_2, H, O, O_2, OH, H_2O, HO_2, H_2O_2, CH_2, CH_2*, CH_3, CH_4, CO, CO_2, HCO, CH_2O, CH_3O, C_2H_2, C_2H_3, C_2H_4, C_2H_5, HCCO, CH_2CO, C_2H_3O, N_2	C, CH, CH_2OH, CH_3OH, C_2H, C_2H_6, HCCOH, AR, C_2O, C_3H_2, C_3H_3, PC_3H_4, AC_3H_4, C_4H, C_4H_2, H_2C_4O, n-C_4H_3, i-C_4H_3, C_4H_4, n-C_4H_5, i-C_4H_5, C_4H_6, C_4H_6-12, C_5H_2, C_5H_3, C_6H, C_6H_2, C_6H_3, l-C_6H_4, c-C_6H_4, n-C_6H_5, i-C_6H_5, l-C_6H_6, n-C_6H_7, i-C_6H_7, c-C_6H_7, C_6H_8, A1, A1-, C_6H_5O, C_6H_5OH, C_5H_6, C_5H_5, C_5H_5O, C_5H_4OH, C_5H_4O	CH_2*
24-species	H_2, H, O, O_2, OH, H_2O, HO_2, H_2O_2, CH_2, CH_3, CH_4, CO, CO_2, HCO, CH_2O, CH_3O, C_2H_2, C_2H_3, C_2H_4, C_2H_5, HCCO, CH_2CO, C_2H_3O, N_2		
19-species	H_2, H, O, O_2, OH, H_2O, HO_2, CH_3, CO, CO_2, HCO, CH_2O, CH_3O, C_2H_2, C_2H_3, C_2H_4, CH_2CO, C_2H_3O, N_2		H_2O_2, CH_2, CH_2*, CH_4, C_2H_5, HCCO

Further study has been conducted to identify the importance of individual species that are removed from the 24-species skeletal mechanism and their associated reactions. It is found that the deletion of C_2H_5 and CH_4 from the 24-species skeletal mechanism causes significant error in ignition delay times at temperatures below 1200 K, as shown in Fig. 4(a). The exclusion of HCCO leads to under-estimation of flame speed in the entire fuel/air equivalence ratio range—as demonstrated in Fig. 4(b)—since HCCO is a critical species for the formation of CO and CO_2 and for the heat release. CH_2 is the only species that may be deleted without affecting the overall accuracy of the skeletal mechanism. Figures 5(a) and 5(b) present the comparison of the ignition delay times and flame speeds calculated by the detailed mechanism and the 23-species skeletal mechanism (where CH_2 is removed from the 24-species skeletal mechanism). Maximum discrepancies of 24% and 5% are found in Fig. 6 for ignition delay time and laminar flame speed predictions, respectively. The above study reveals that with certain accuracy (less than 30% in the error of ignition delay times and less than 15% in the error of laminar flame speeds), there exists a minimum number of species for skeletal mechanisms.

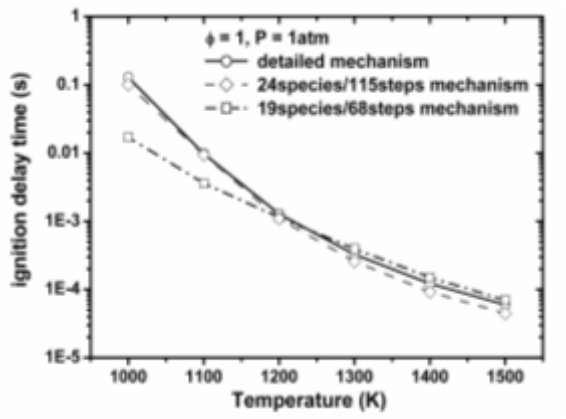

(a)

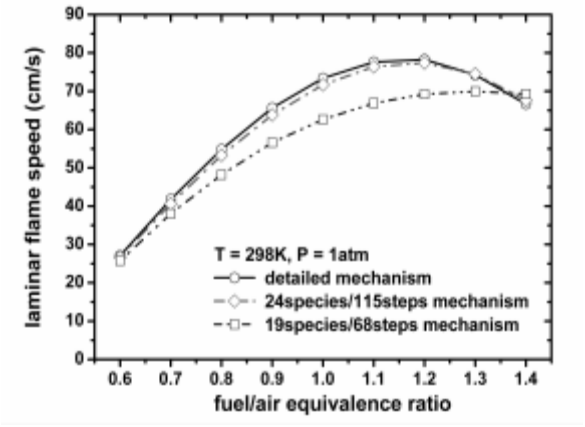

(b)

Fig. 3 Comparisons of the detailed mechanism and the 24-species and the 19-species skeletal mechanisms. (a): ignition delay time; (b): laminar flame speed

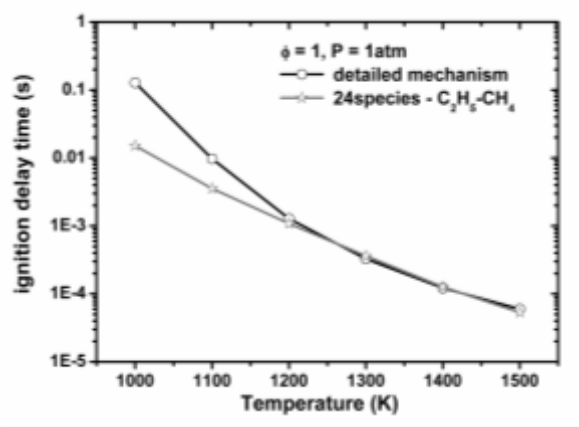

(a)

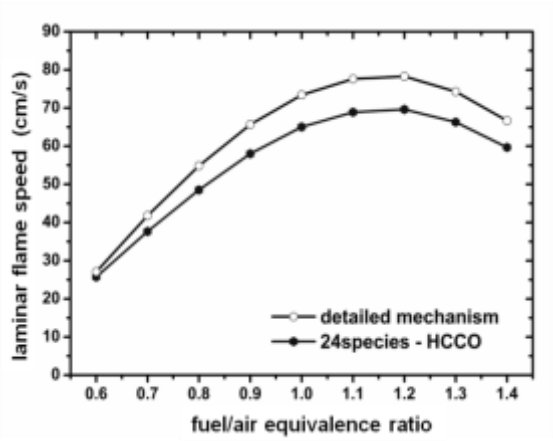

(b)

Fig. 4 Comparison of the detailed mechanism with the skeletal mechanisms resulted by removing species from the 24-species skeletal mechanism. (a): ignition delay time; (b): laminar flame speed

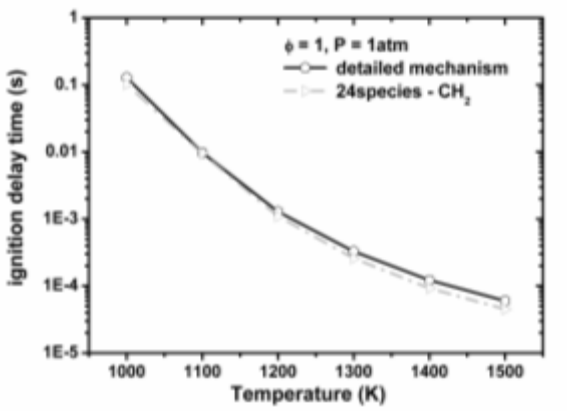

(a)

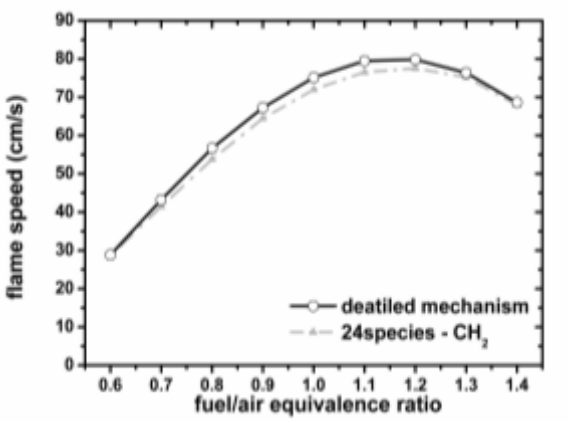

(b)

Fig. 5 Comparison of the detailed mechanism with the skeletal mechanism resulted by removing CH_2 from the 24-species skeletal mechanism. (a): ignition delay time; (b): laminar flame speed

3.2 Skeletal mechanism of n-alkanes with low temperature chemistry

The detailed mechanism for C_8–C_{16} alkanes developed by Westbrook et al. [3] is reduced to show the performance of DRGEPSA for large-size mechanisms. The detailed mechanism consists of 2115 species and 8157 reaction steps and it has been validated to be accurate at a temperature range of 600–1500 K and at pressures less than 30 atm as described in Ref. [3]. The inclusion of low-temperature chemistry (600–900 K) increases the mechanism size. Using n-dodecane as the fuel and with a stoichiometric n-dodecane/air mixture, an input temperature range of 800–1500 K, an input pressure of 1 atm, and the error limit δ_{EP} set as 30% for the full temperature range (resulting in ε_{EP} = 0.0003), a skeletal mechanism with 249 species and 910 reaction steps is obtained. Fig. 6 shows the comparison of ignition delay times obtained with the detailed and the skeletal mechanisms. It is seen in the full temperature range of 600–1500 K that the two curves agrees well with each other with a maximum difference of only 26%. However, a skeletal mechanism of 249 species is still considerably large when desired for use in multidimensional computations. For many supersonic combustor flows in scramjets, the static temperature at the combustor entrance has already risen to a high value due to the compression effect of the scramjet inlet [cf. 33, 34]. If considering only high-temperature chemistry (> 900 K), such skeletal mechanisms can be further reduced.

Figure 7 shows the ignition delay times predicted with two skeletal mechanisms. Both skeletal mechanisms have much fewer species (65 species and 48 species) than the previous one (249 species). As shown in Fig. 8, in the high temperature range (1000–1500 K), both smaller skeletal mechanisms give relatively satisfactory results compared with the detailed mechanism, but in the lower temperature range (≤ 900 K), they are no longer able to correctly represent the detailed mechanism. It is also found that the 65-species skeletal mechanism performs better than the 48-species skeletal mechanism at temperatures larger than 1200 K. For the 48-species skeletal mechanism, an error of 50% is observed at temperatures close to 1300 K, beyond the desired error tolerance of 30%.

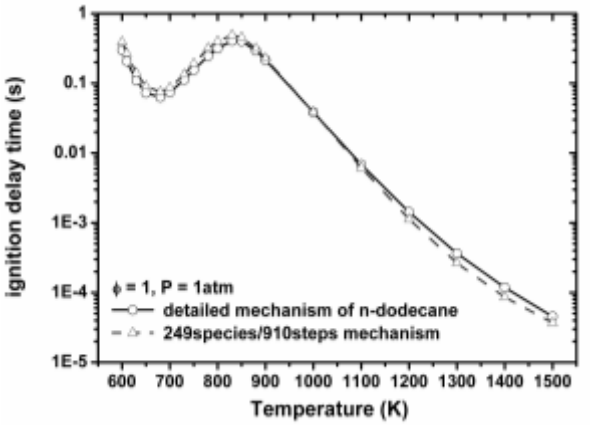

Fig. 6 Variation of ignition delay time with temperature obtained by the detailed mechanism and the 249-species skeletal mechanism

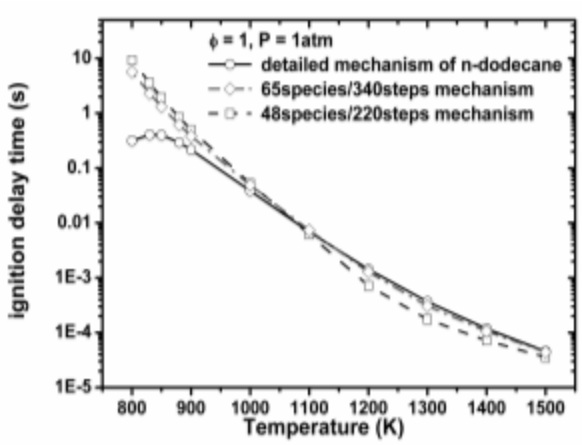

Fig. 7 Variation of ignition delay time with temperature obtained by the detailed mechanism and the 65-species and 48-species skeletal mechanisms

3.3 Skeletal mechanism of a kerosene surrogate

Finally, a detailed mechanism of a kerosene surrogate is tested. This detailed mechanism taken from Dagaut [28] considered three fuel components (n-decane, n-propylbenzene, and n-propylcyclohexane) in the surrogate mixture and consisted of 207 species and 1592 reaction steps. The detailed mechanism has been validated with comparisons to the experimental data of JSR (jet-stirred reactor). In light of the study of Fan et al. [34], a three-component surrogate, containing 49% n-decane, 44% n-propylcyclohexane, and 7% n-propylbenzene in molar percentages, which has different composition from that of Dagaut [28], is used in order to better model China No. 3 aviation kerosene.

It is worth noting that the detailed mechanism of Dagaut [28] included mainly high-temperature chemistry, and hence it is only valid in the high-temperature regime, i.e., temperatures should be no less than 1000 K. Figure 8 shows the ignition delay times at two pressures predicted by the detailed mechanism and a skeletal one with 72 species and 429 reaction steps. The skeletal mechanism is obtained with a stoichiometric surrogate/air mixture, an input temperature range of 1100–1400 K, an input pressure of 1 atm, and the error limit δ_{EP} set as 30% (resulting in $\varepsilon_{EP} = 0.055$). It is also noted that the two pressures of 1 atm and 6 atm in Fig. 8 represent the typical lower and upper limit values for supersonic combustor flows [cf. 33, 34]. Figure 8 indicates that the 72-species skeletal mechanism works quite well and the maximum discrepancy with the detailed mechanism is 31%. By further decreasing the input temperature range, the size of the skeletal mechanism can be further decreased to 66 species and 63 species. Figures 9(a) and 9(b) present the ignition delay results obtained using these two skeletal mechanisms at pressures of 1 atm and 6 atm. The 66-species mechanism can still give relatively good results of ignition delay times with a maximum discrepancy of 33%. The 63-species mechanism, however, predicts some different results, especially in the temperature range of 1000–1200 K, where the maximum discrepancy may reach 200%. The present results also indicate that the accuracy of the skeletal mechanism decreases with decreasing number of species, and hence a minimum number of species should be retained to ensure a desirable accuracy.

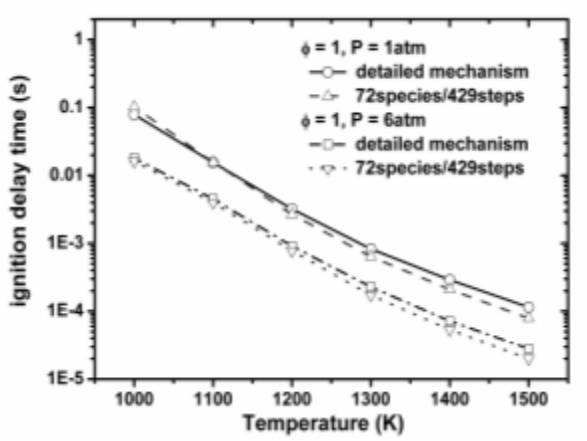

Fig. 8 Comparisons of ignition delay times obtained with the detailed mechanism and the 72-species skeletal mechanisms at two pressures

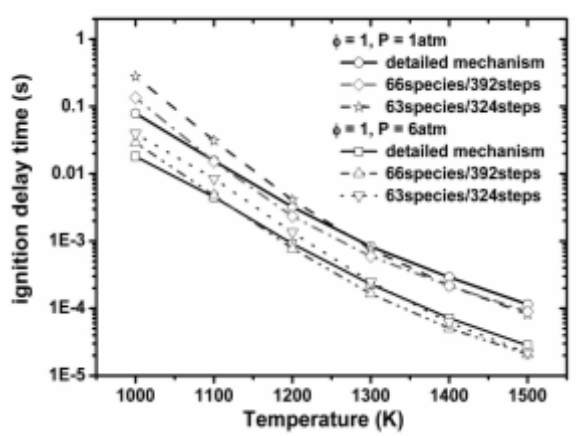

Fig. 9 Comparisons of ignition delay times obtained with the detailed mechanism as well as the 66-species and the 64-species skeletal mechanisms at two pressures

4. Conclusions

In this paper, the methodology of directed relation graph with error propagation and sensitivity analysis (DRGEPSA), proposed by Niemeyer et al. [21], is described. Using DRGEPSA, the detailed mechanism of ethylene, containing 71 species and 395 reaction steps, is reduced to several skeletal mechanisms with different error thresholds. With comparisons of ignition delay times and laminar flame speeds calculated between the skeletal mechanisms and the detailed mechanism, it is found that the 25 species and 131 steps mechanism can accurately match the detailed reaction mechanism with a maximum error percentage of only 7% for ignition delay times and 5% for laminar flame speeds. The 24 species and 115 steps skeletal mechanism is also accurate enough, but with a larger error percentage of 25%. Further reduction leads to the 19 species and 68 steps skeletal mechanism. However, it gives poor results and is no longer able to represent the correct combustion process.

Reduction of a detailed mechanism for n-dodecane combustion including the low temperature chemistry is then studied. The original detailed mechanism with 2115 species and 8157 reaction steps can be reduced to a much smaller one with 249 species and 910 steps, while still retaining good accuracy. If considering high-temperature applications (temperatures higher than 1000 K), the detailed mechanism can be simplified to much smaller mechanisms with only 65 species and 340 steps or 48

species and 220 steps.

Finally, a detailed mechanism of a three-component kerosene surrogate, having 207 species and 1592 reaction steps, is reduced using varying levels of accuracy. It is found that skeletal mechanisms with 72 species and 429 steps, and 66 species and 392 steps, are capable of obtaining results close to those of the detailed mechanism. It is also shown that a smaller skeletal mechanism with 63 species and 324 steps is not able to give correct results due to the loss of some critical radicals such as C_4H_6.

The chemical kinetic mechanism is recognized as one of the most critical elements for accurate and effective numerical simulation of supersonic or turbulent combustion, especially for unsteady problems involving, e.g., ignition, extinction, and flame propagation. Reaction mechanisms can be effectively used in computations only after they are reduced to an acceptable size for a given computational capacity, while at the same time retaining the desired accuracy. Thus, the present work is expected to be helpful for the application of realistic chemistry of hydrocarbon fuels to numerical simulations of turbulent or supersonic combustion.

Acknowledgment This work is funded by Natural Science Foundation of China under Contract No. 11172309. The authors would like to thank Professor Gong Yu of Chinese Academy of Sciences for his help in this work. CJS is also supported by the China's Programme of Introducing Talents of Discipline to Universities – 111 Project under Grant No. B08009 and the Thousand Talents Program.

References

1. Wang, H. and Laskin, A.: A Comprehensive Kinetic Model of Ethylene and Acetylene Oxidation at High Temperatures, Progress Report for an AFOSR New World Vista Program (1998)
2. Curran, H., Gaffuri, P., Pitz, W. et al.: A Comprehensive Modeling Study of n-Heptane Oxidation, Combustion and Flame **114**, 149-177 (1998)
3. Westbrook, C.K., Pitz. W.J., Herbinet, O. et al.: A Comprehensive Detailed Chemical Kinetic Reaction Mechanism for Combustion of N-alkane Hydrocarbons from N-octane to N-hexadecane, Combustion and Flame **156**, 181-199 (2009)
4. Tishkoff, J.M., Drummond, J.P., Edwards, T.: Future Directions of Supersonic Combustion Research, Air Force/NASA Workshop on Supersonic Combustion, AIAA Paper 1997-1017 (1997).
5. Lu, T., and Law, C.K.: Toward accommodating realistic fuel chemistry in large-scale computations, Progress in Energy and Combustion Science **35**, 192-215 (2009)
6. Pope, S.B.: Small scales, many species and the manifold challenges of turbulent combustion, Proceedings of the Combustion Institute **34**, 1-31 (2013)
7. Rabitz, H., Kramer, M., Dacol, D.: Sensitivity Analysis in Chemical Kinetics, Annual Review of Physical Chemistry **34**, 419-461 (1983)
8. Turányi,T.: Sensitivity analysis of complex kinetic systems, Tools and applications, Journal of Mathematical Chemistry **5**, 203-248 (1990)
9. Lam, S.H.: Using CSP to Understand Complex Chemical Kinetics, Combustion Science and Technology **89**, 375–404 (1993)
10. Peters, N., Rogg, B.: Reduced Kinetic Mechanisms for Applications in Combustion Systems, Springer-Verlag, Berlin, (1993)
11. Chen, J.-Y.: Development of Reduced Mechanisms for Numerical Modelling of Turbulent Combustion, Workshop on Numerical Aspects of Reduction in Chemical Kinetics, CERNICS-ENPC，Cite Descartes, Champus sur Marne, France, (1997)
12. Montgomery, C.J. Zhao, W. Tam, C.-J. et al.: CFD Simulation of a 3-D Scramjet Flameholder Using Reduced Chemical Kinetic Mechanisms, AIAA 2003-3874 (2003).
13. Zhong, F.-Q., Chen L.-H., Li F. et al.: Numerical Simulation of Ignition and Combustion of Ethylene in a Supersonic Model Combustor with a Reduced Kinetic Mechanism, Combustion Science and Technology **185,** 548-563 (2013)
14. Pope, S.B.: Computationally efficient implementation of combustion chemistry using *in situ* adaptive

tabulation, Combustion Theory and Modelling **1**, 41–63 (1997)

15. Lu, L., Pope, S.B.: An improved algorithm for *in situ* adaptive tabulation, Journal of Computational Physics **228**, 361–386 (2009)
16. Pope, S.B., Ren, Z.: Efficient implementation of chemistry in computational combustion, Flow, turbulence and combustion **82**, 437-453 (2009)
17. Lu, T., Law, C.K.: A Direct Relation Graph for Mechanism Reduction, Proceedings of the Combustion Institute **30**, 1333-1341 (2005)
18. Lu, T., Law, C.K.: On the Applicability of Directed Relation Graphs to the Reduction of Reaction Mechanisms, Combustion and Flame **146**, 472-483 (2006)
19. Lu, T., Law, C.K.: Linear Time Reduction of Large Kinetic Mechanisms with Directed Relation Graph: N-heptane and iso-octane, Combustion and Flame **144**, 24-36 (2006)
20. Pepiot-Desjardins, P., Pitsch, H.: An Efficient Error-propagation-based Reduction method for large chemical kinetic mechanisms, Combustion and Flame **154**, 67-81 (2008)
21. Niemeyer K.E., Sung, C.-J., Raju, M.P.: Skeletal Mechanism Generation for Surrogate Fuels Using Directed Relation Graph with Error Propagation and Sensitivity Analysis, Combustion and Flame **157**, 1760-1770 (2010)
22. Niemeyer K.E., Sung, C.-J.: On the Importance of Graph Search Algorithms for DRGEP-based Mechanism Reduction Methods, Combustion and Flame **158**, 1439-1443 (2011)
23. Liang, L., Stevens, J.G., Farrell, J.T.: A dynamic adaptive chemistry scheme for reactive flow computations, Proceedings of the Combustion Institute **32**, 527-534 (2009)
24. Liang, L., Stevens, J.G., Raman, S. et al.: The use of dynamic adaptive chemistry in combustion simulation of gasoline surrogate fuels, Combustion and Flame **156**, 1493-1502 (2009)
25. Yang, H., Ren, Z., Lu, T. et al.: Dynamic adaptive chemistry for turbulent flame simulations, Combustion Theory and Modelling **17**, 167-183 (2013)
26. Shi, Y., Liang, L., Ge, H.-W. et al.: Acceleration of the chemistry solver for modeling DI engine combustion using dynamic adaptive chemistry (DAC) schemes, Combustion Theory and Modelling **14**, 69-89 (2010)
27. Ren, Z., Liu, Y., Lu, T. et al.: The use of dynamic adaptive chemistry and tabulation in reactive flow simulations, Combustion and Flame **161**, 127-137 (2014)
28. Dagaut P.: On the kinetics of hydrocarbons oxidation from natural gas to kerosene and diesel fuel, Phys.Chem.Chem.Phys. **4**, 2079-2094 (2002)
29. Zheng X.L., Lu T.F., Law C.K.: Experimental Counterflow Ignition Temperatures and Reaction Mechanisms of 1, 3-Butadiene, Proc.Combust.Inst.**31**, 367-375 (2007)
30. Saxena S., Kahandawala, M.S.P., Sidhu, S.: A Shock Tube Study of Ignition Delay in the Combustion of Ethylene, Combustion and Flame **158**, 1019-1031 (2011)
31. Gibbs G.J., Calcote H.F.: Effect of Molecular Structure on Burning Velocity, J. Chem. Eng. Data **4**, 226–237 (1959)
32. Egolfopoulos, F.N., Zhu D.L., Law, C.K.: Experimental and Numerical Determination of Laminar Flame Speeds: Mixtures of C2 Hydrocarbons with Oxygen and Nitrogen, The 23rd Symposium (International) on Combustion, **23**, 471-478 (1991)
33. Zhong, F.-Q., Fan X.-J., Yu G. et al.: Performance of supersonic model combustors with staged injections of supercritical aviation kerosene, Acta Mechanica Sinica **26**, 661-668 (2010)
34. Fan, X.-J., Yu, G., Li, J.-G. et al.: Investigation of Vaporized Kerosene Injection and Combustion in a Supersonic Model Combustor, Journal of Propulsion and Power **22**, 103-110 (2006)